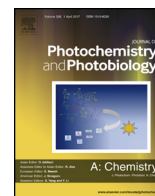




Contents lists available at ScienceDirect

Journal of Photochemistry and Photobiology A: Chemistry

journal homepage: www.elsevier.com/locate/jphotochem

Line defect Ce³⁺ induced Ag/CeO₂/ZnO nanostructure for visible-light photocatalytic activity

R. Saravanan^a, Shilpi Agarwal^b, Vinod Kumar Gupta^{b,c,*}, Mohammad Mansoob Khan^d, F. Gracia^a, E. Mosquera^e, V. Narayanan^f, A. Stephen^{g,*}

^a Department of Chemical Engineering, Biotechnology and Materials, University of Chile, Beauchef 851, 6th floor, Santiago, Chile

^b Department of Applied Chemistry, University of Johannesburg, Johannesburg, South Africa

^c Department of Biological Sciences, King Abdulaziz University, Jeddah 21589, Saudi Arabia

^d Chemical Sciences, Faculty of Science, Universiti Brunei Darussalam, Jalan Tungku Link, Gadong, BE 1410, Brunei Darussalam

^e Departamento de Física, Universidad del Valle, A.A. 25360, Cali, Colombia

^f Department of Inorganic Chemistry, University of Madras, Guindy Campus, Chennai, 600 025, India

^g Department of Nuclear Physics, University of Madras, Guindy Campus, Chennai, 600 025, India

ARTICLE INFO

Article history:

Received 27 October 2017

Received in revised form 7 December 2017

Accepted 8 December 2017

Available online 9 December 2017

Keywords:

Silver nanoparticles

Narrow band gap

Oxygen vacancy

Defects

Photocatalysts

Visible light

ABSTRACT

This article reports, synthesis and characterization of the ternary Ag/CeO₂/ZnO nanostructure which was tested for visible light photocatalytic degradation of industrial textile effluent. The HR-TEM and XPS results confirm the presence of line dislocation linear defect induced oxygen vacancy in the ternary Ag/CeO₂/ZnO nanostructure. The oxygen vacancy creates narrow band gap (2.66 eV) was confirmed by DRS. The ternary Ag/CeO₂/ZnO nanostructure showed superior photocatalytic activity compared with pure ZnO, ZnO/Ag and ZnO/CeO₂ results because of the narrow band gap, surface plasmon resonance (SPR) of Ag nanoparticles, synergistic effects, and defects (Ce³⁺ and oxygen vacancy) in CeO₂ and ZnO.

© 2017 Elsevier B.V. All rights reserved.

1. Introduction

Advancement in nanostructure developments bring out wide range of industrial, health and environmental applications. The nanomaterials acquired have novel properties in which the reactions are carried out by altering the reaction conditions [1–3]. Currently environmental hazard is one of the significant topics of scientific topics of research. There are large number of polluting agents present in the atmosphere due to exceeding world's population which encourages huge number of industries, vehicles and so on. Our day to day life of utilizing polluted air and water does not provide good health benefits, because of the presence of harmful chemicals [4]. Practice of dumping waste waters into the fresh water sources like rivers, streams, lakes and oceans brings about variety of health risks to human beings, plants and animals [4]. Hoffman et al. has reported that more than 70% of waste disposal includes toxic chemicals, the primary cause for the

contamination of underground water resources [5]. One of the major reasons for water pollution is untreated industrial textile dyes, since it is being released into most of the water resources without any kind of treatment processes. It creates harmful environment and hence several diseases to human beings, plants and animals [4–8].

In recent decades, researchers are putting their efforts to utilize various semiconductor nano metal oxides for photocatalytic degradation process in the waste water treatment [5–9]. Photocatalytic degradation process is gaining much attention in degrading the pollutants by the most inexpensive route, because it requires small amount of catalysts, no need of special equipment and requires very less energy for generation of electrons and holes [5,7]. Apart from various metal oxides, zinc oxide (ZnO) is a cost effective large band gap semiconductor used for versatile applications due to its fascinating properties like non-toxicity, chemical and physical stability [10–12]. One of the disadvantage of ZnO is its large band gap that inhibits to make electrons and holes during the photocatalytic processes under visible light illumination [13,14]. Recently, modification of ZnO by various methods to utilize the ZnO based photocatalyst under visible light irradiation [13,14]. Earlier, we had described that in ZnO/CeO₂ nanocomposite

* Corresponding authors.

E-mail addresses: vinodg@uj.ac.za, vinodfcy@gmail.com (V.K. Gupta), stephen_arum@hotmail.com (A. Stephen).

the synergetic effect between ZnO and CeO₂ semiconductor stimulated the formation of more electrons and holes during visible light irradiation, which promotes superior degradation of methylene blue in 150 min [15]. In case of ZnO/Ag nanocomposite the surface defect has induced to inhibit electron-hole pairs recombination during the photocatalytic process, which led to improve the efficiency of the degradation of MB in 2 h under visible light irradiation [13].

Therefore, the main objective of this work is to synthesize a novel nanostructure which can be used to degrade dyes and industrial textile effluent (real samples) under visible light irradiation, enhance the photocatalytic degradation efficiency and minimize the irradiation time compared with previously reported photocatalysts [13,15]. The ternary Ag/CeO₂/ZnO nanostructure was synthesized by an inexpensive thermal decomposition method. The morphological, structural and chemical composition of the photocatalyst was characterized by various standard techniques. Furthermore, the ternary Ag/CeO₂/ZnO nanostructure was efficiently used to degrade the model dyes such as MO, MB and Phenol as well as industrial textile effluent (real sample analysis) under visible light irradiation.

2. Experimental procedure

2.1. Materials

Silver acetate, cerium (III) acetate hydrate, zinc acetate dehydrate, methylene blue (MB) and methyl orange (MO) were purchased from Sigma-Aldrich. All the aqueous solutions were prepared using double distilled water.

2.2. Synthesis of ternary Ag/CeO₂/ZnO nanostructure as photocatalyst

The synthesis of ternary Ag/CeO₂/ZnO nanostructure was based on the vapor to solid mechanism [16]. Based on this mechanism, the synthesis procedure of ternary Ag/CeO₂/ZnO nanostructure as follows: weight ratio (10:10:80) of silver acetate, cerium (III) acetate hydrate and zinc acetate dihydrate (raw materials) were mixed together and grounded for ~3 h using a mortar (agate). The grounded reactants (raw materials) were reserved into an alumina crucible and calcined with the use of muffle furnace at 350 °C for 3 h. At first, the mixed reactants get dehydrated (~100 °C to 150 °C) and gives anhydrous mixed acetates. Further, the temperature was slowly rising (150 °C – 350 °C). In this duration, the mixed acetates was decomposed well along with vaporization gets started. Moreover, the muffle furnace temperature was reduced slowly (4 °C per min), the vaporized materials get condensed and settled in a crucible at room temperature. Finally, we got ternary Ag/CeO₂/ZnO nanostructure powder which was used for characterization and photocatalytic degradation of model dyes and industrial textile effluent (real sample analysis).

2.3. Photocatalytic experiment

In this work, we have preferred industrial textile (real sample) effluent and two azo dyes (MO and MB) and phenol solution for degradation under visible light irradiation. The degradation of colorants is extremely important since industrial textile waste water comprises with a lot of colored and harmful substances [17]. The preparation of dyes solution and industrial textile effluent procedures were adopted from previous report¹³. In short, initially, 500 mg of photocatalyst was mixed with 500 mL of aqueous solutions of pollutants (MO, MB, Phenol and industrial textile dye) in a 600 mL cylindrical vessel. The solutions were again stirred in the dark for 30 min to complete the adsorption and desorption equilibrium on the photocatalysts. The source of the visible light

was a solar simulator (SCIENCETECH, model No: SF300B, along with AM 1.5G filter which is due to given standard solar spectrum. The illumination intensity of a light irradiation at the sample surface was ~100 mW/cm². Initial (without irradiation) and irradiated samples were analyzed using UV–vis spectrophotometer for dye degradation and TOC measurements for real textile effluent.

2.4. Characterization details

The structure and crystallite size of the prepared ternary Ag/CeO₂/ZnO nanostructure was determined by X-ray diffractometer (Rich Seifert 3000, Germany) using Cu K_{α1} radiation with λ = 1.5406 Å. The presence of elements in the photocatalyst and their oxidation states were examined using X-ray photoelectron spectroscopy (XPS, DRA 400–XM1000 OMICRON, ESCA⁺, Omicron Nanotechnology, Germany). Specific surface area was calculated using Brunauer–Emmett–Teller (BET, Micromeritics ASAP 2020, USA) equation. Surface morphology, elemental analysis and energy dispersive X-ray spectroscopy (EDS) analyses were carried out using field emission scanning electron microscope (FE-SEM, HITACHI-SU6600, Hitachi, Japan). The microstructure, interfaces and elemental mapping was performed by high resolution transmission electron microscope and scanning transmission electron microscope (HR-TEM and STEM, Tecnai F20-FEI, USA). The optical band gap of the photocatalyst was calculated from diffuse reflectance spectra (DRS) by using a UV–VIS–NIR spectrophotometer (VARIAN CARY 5E, USA). The photocatalytic degradation activities were measured using UV–vis spectrophotometer (RX1, Perkin – Elmer, USA).

3. Results and discussion

The X-ray diffraction pattern of ternary Ag/CeO₂/ZnO nanostructure is depicted in Fig. 1. All the characteristic peaks are indexed perfectly with the JCPDS files. From Fig. 1, it was identified that the diffraction pattern consists of ZnO, Ag along with CeO₂ peaks. The XRD pattern of ZnO shows (100), (002), (101), (102), (110), (103), (112), (201) and (200) planes which describe the hexagonal structure (JCPDS No. 79-0208) along with (111), (200), and (202) planes which corresponds to the cubic structure of Ag (JCPDS No. 89-5899) which are represented by '#' in Fig. 1. In addition, the '*' mark represented the (111) and (200) planes for cubic structure of CeO₂, which is in accordance with the JCPDS. No.

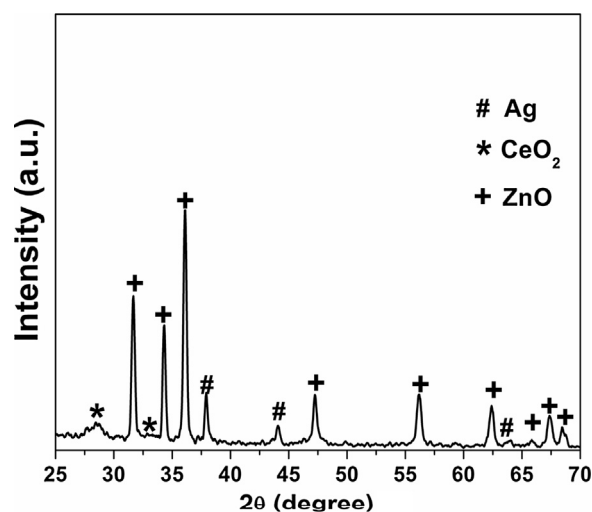


Fig. 1. XRD patterns of ternary Ag/CeO₂/ZnO nanostructure.

65–2975. No other impurities were detected in the XRD pattern. Therefore, XRD result has confirmed the synthesis of ternary Ag/CeO₂/ZnO nanostructure.

The surface chemical composition and chemical states of the ternary Ag/CeO₂/ZnO nanostructure was examined by XPS and its survey spectrum is shown in Fig. 2(a) which confirms that it consists of Ag, Ce, Zn, O and C elements. The binding energy (BE) values at 1021.1 eV and 1044.3 eV represents Zn 2p_{3/2} and Zn 2p_{1/2} peaks (Fig. 2(b)) for Zn in ternary Ag/CeO₂/ZnO nanostructure which indicates that Zn exists in +2 oxidation state [13]. The high resolution XPS spectrum of Ag is shown in Fig. 2(c) which shows peaks of Ag 3d_{5/2} and Ag 3d_{3/2} at BE 366.1 eV and 372.1 eV, respectively, which are core level Ag 3d spectra of the silver nanoparticles (AgNPs) with ~6.0 eV splitting between the two peaks, which is attributed to the complete reduction of Ag⁺ to Ag⁰ [13,18]. However, the BE of Ag 3d_{5/2} shifted to a lower BE compared to the corresponding value of the synthesized pure metallic Ag (the BE of Ag⁰ is ~368.2 eV) [17]. This is attributed to the formation of

AgNPs in the nanostructure¹⁸. The high resolution scanning XPS spectrum of cerium along with the satellite peaks are presented in Fig. 2(d). The binding energies are 881.7 eV and 905.8 eV for Ce 3d_{5/2} and Ce 3d_{3/2} peaks which confirm that cerium exists in +4 oxidation state in the ternary Ag/CeO₂/ZnO nanostructure [19].

In the XPS analysis also confirms the presence of both Ce⁴⁺ and Ce³⁺ in ternary Ag/CeO₂/ZnO nanostructure, which is due to the formation of more defects and/or an amorphous phase of Ce₂O₃. As indicated by XPS the ternary Ag/CeO₂/ZnO nanostructure contained Ce³⁺ and defects which might lead to the formation of a surface state energy band of oxygen. The oxygen adsorption, desorption and diffusion processes may occur easily on the surface of the ternary Ag/CeO₂/ZnO nanostructure, that can greatly enhance their optical properties and imparts visible light photocatalytic activity⁸. Therefore, a new Fermi energy level in ternary Ag/CeO₂/ZnO nanostructure is formed, indicating a strong interaction between Ag, CeO₂ and ZnO nanoparticles¹⁸. Once the AgNPs are formed along with the CeO₂, and ZnO, electron transfer

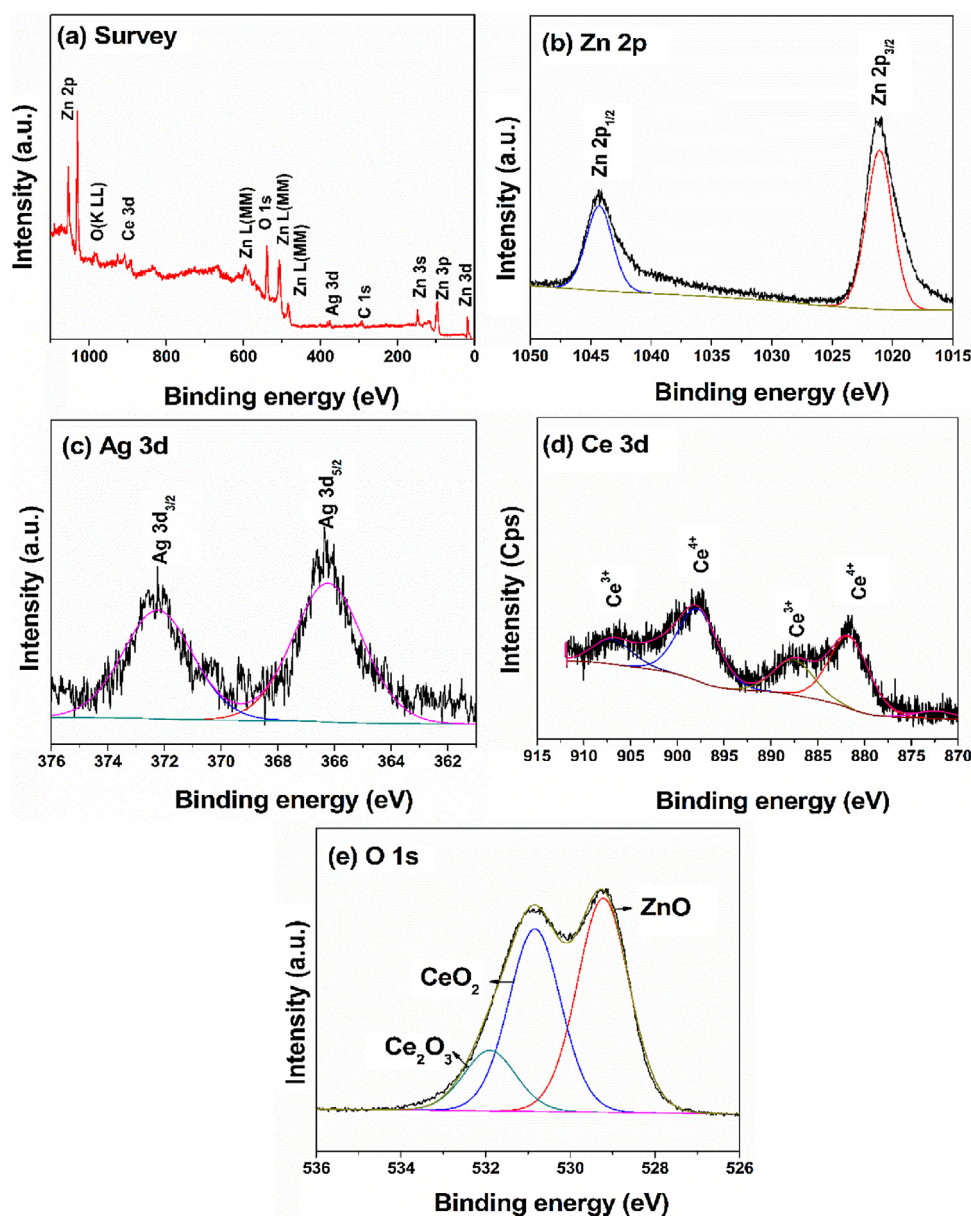


Fig. 2. XPS spectra of ternary Ag/CeO₂/ZnO nanostructure (a) Survey spectrum, (b) HR-XPS spectrum of Zn 2p, (c) HR-XPS spectrum of Ag 3d, (d) HR-XPS spectrum of Ce 3d, and, (e) HR-XPS spectrum of O 1s.

occurs from Ag to CeO₂ to ZnO because the work function of silver (4.26eV) is smaller than that of CeO₂ (4.69eV) and ZnO (5.20eV) [13,18,20–21]. Fig. 2(e) shows three different kinds of oxygen (529.2, 530.8 and 531.9eV) on the surface of ternary Ag/CeO₂/ZnO nanostructure which are associated with Zn²⁺, Ce⁴⁺, and Ce³⁺ [6,8,22]. Hence, the XPS result has confirmed the synthesis of ternary Ag/CeO₂/ZnO nanostructure and there was no any other impurities found in the samples. Further, the determination of particle size and morphology of the ternary Ag/CeO₂/ZnO nanostructure are the necessary parameters, because these parameters plays vital role to get the effective efficiency during the photocatalytic activity.

The morphological analysis of ternary Ag/CeO₂/ZnO nanostructure was carried out by FE-SEM. For the comparison purpose, the pure ZnO nanorods were synthesized by the same method at same reaction condition and its FE-SEM and EDS are shown by Fig. 3a and a'. The FE-SEM image of ternary Ag/CeO₂/ZnO nanostructure specifies the presence of aggregated nanorods along with spherical shaped nanoparticles which are shown in Fig. 3(b). From the FE-SEM images, it was clearly represented that when compared with pure ZnO nanorods (Fig. 3(a)), the size of ZnO nanorods present in the ternary Ag/CeO₂/ZnO nanostructure was smaller, which may be due to Ag and CeO₂ nanoparticles which inhibits the growth of nanorods due to its nucleation effect [23].

The EDS pattern (Fig. 3b') confirms the presence and synthesis of pure ZnO and ternary Ag/CeO₂/ZnO nanostructure with their constituent elements. Due to large amount of aggregation, we could not find out the exact size of the ternary Ag/CeO₂/ZnO nanostructure from the FE-SEM. Therefore, we performed TEM analysis to get the exact size, morphology, interface and d-spacing of ternary Ag/CeO₂/ZnO nanostructure.

The TEM image of ternary Ag/CeO₂/ZnO nanostructure is shown in Fig. 4(a) which clearly represented the presence of ZnO nanorods along with Ag and CeO₂ nanoparticles which are in accordance with FE-SEM results. The length of the nanorods is

around 100 to 150nm and the diameter is in the range of 20 – 35nm. From the HR-TEM (Fig. 4(b)), we determined d-spacing value of each elements.

The crystallites exhibited (111) plane of Ag showing cubic structure, (200) plane corresponds to cubic structure of CeO₂ and (101) planes for hexagonal structure of ZnO. From the close observation of HR-TEM (Fig. 4(b)) represents line dislocation linear defect (Fig. 4c) because of formation of very small amount of amorphous Ce₂O₃, which promotes oxygen vacancies due to the nucleation effect [8,13,24]. Amorphous regions are also observed (Fig. 4c) around the crystalline particles, suggesting the presence of amorphous Ce₂O₃ in the samples. Hence, the results of FE-SEM and TEM analyses clearly shows formation of the ternary Ag/CeO₂/ZnO nanostructure which are smaller than the pure ZnO. The particles position in the ternary nanocomposite is essential parameter to find the interfaces of the synthesized ternary Ag/CeO₂/ZnO nanostructure which were identified by STEM; the parallel bright and dark field images which are shown in Fig. S1. The elemental mapping (Fig. S2) were carried out based on STEM image and their spread uniformly rather than being separated individually or edged. These observations confirm the effective interfaces which modified the electronic-structure and facilitate charge-carrier transfer between Ag, CeO₂ and ZnO [25].

The BET measurement values also in agreement with the TEM observation. The ternary Ag/CeO₂/ZnO nanostructure (39.2m²g⁻¹) shows 4.5 times greater surface area than the pure ZnO nanorods (8.7m²g⁻¹), due to the nucleation effect between Ag, CeO₂ and ZnO that promotes the smaller size of ternary system. Wang et al. observed similar phenomenon for silver doped into ZnO/SnO₂ system [26].

The optical band gap of the prepared materials were analyzed by using Kubelka-Munk function. It was clearly displayed in Fig. 5(a), the nanocomposite materials indicate narrow bandgap (2.66eV) when compared with pure ZnO (3.31eV). The absorbance band edge (Fig. 5(b)) of the nanocomposite is wider because it

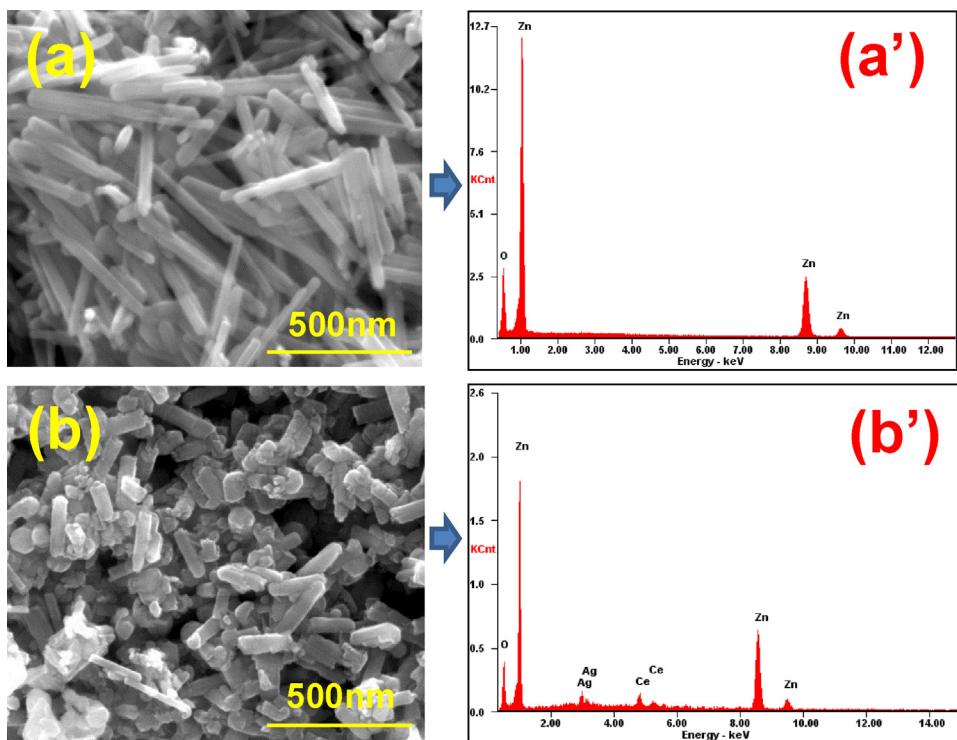


Fig. 3. The FE-SEM images and respective EDS spectra of (a and a') ZnO, and, (b and b') ternary Ag/CeO₂/ZnO nanostructure.

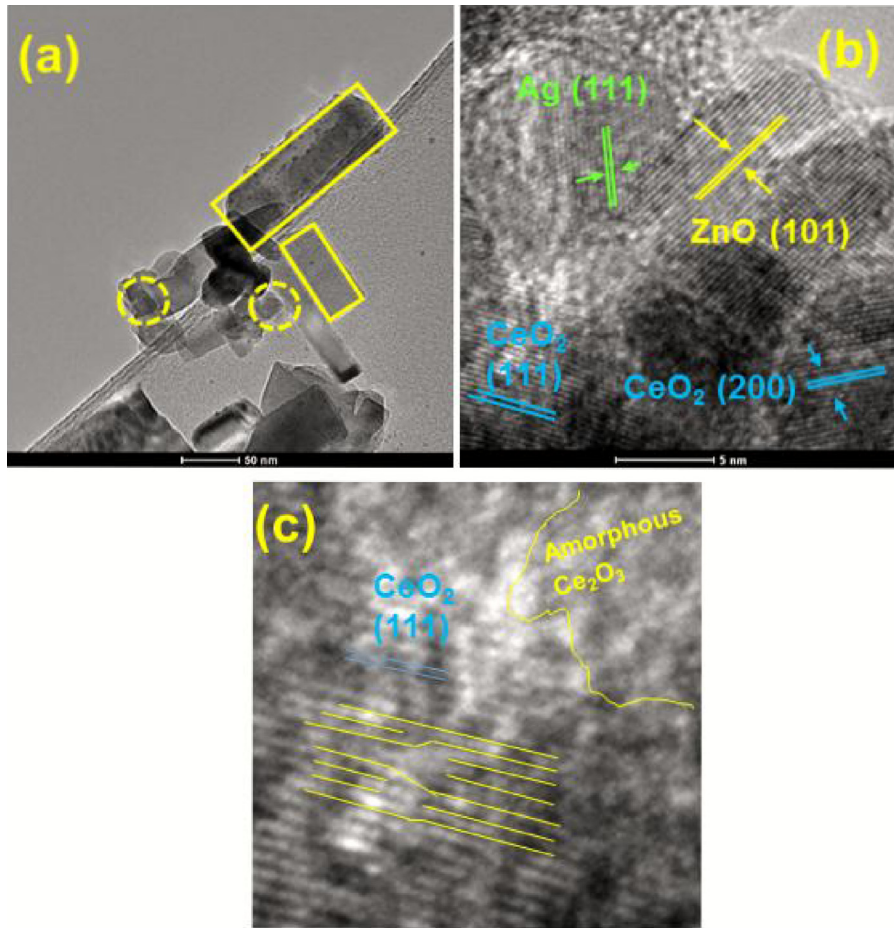


Fig. 4. (a) TEM image, (b) HR-TEM image, and, (c) line dislocation pattern of ternary Ag/CeO₂/ZnO nanostructure.

contains Ag, CeO₂ and amorphous Ce₂O₃, whereas the pure ZnO has a very sharp band edge [27]. This wider band edge is due to oxygen vacancies which generate intermediate states and so the bandgap is narrow [6,13]. The reflection of TEM image has evidently showed the oxygen vacancies present in this nano-composite system due to line defect. This observation is of good agreement with the previous reports [6,13,28]. On the other hand, the improved photocatalytic activity mostly depends on the prevention of electrons and holes combination [16,18]. The photoluminescence results (Fig. S3) were evidently indicated that the intensity of Ag/CeO₂/ZnO is suggestively low while compared

with pure ZnO, Ag/ZnO and CeO₂/ZnO materials. The lowering intensity specified that the reduced recombination, which is highly favored for enhanced photocatalytic activity [16]. Therefore the ternary material is expected degrading the solution under visible light condition.

3.1. Visible light photocatalytic degradation

Some of the earlier reports clearly showed that the ZnO have a wide band gap, hence during the visible light irradiation, it was unable to create sufficient electrons and holes for photocatalytic

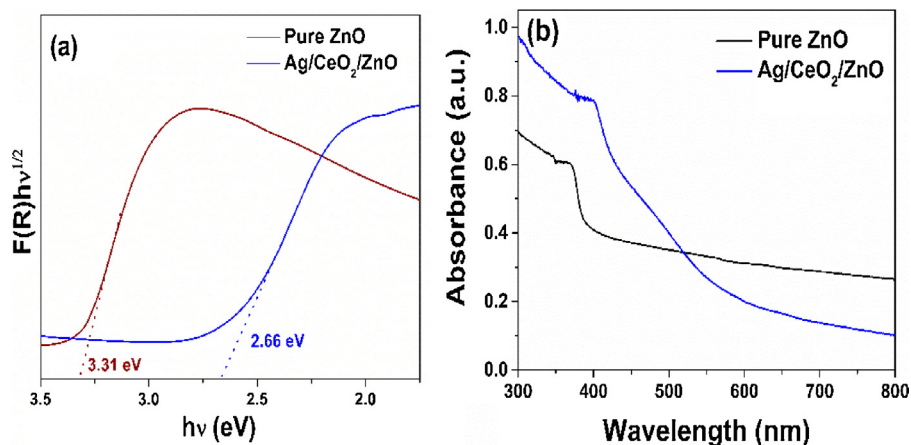


Fig. 5. (a) K-M function $F(R)hv^{1/2}$ vs hv plot, and, (b) UV-vis absorbance of the ternary Ag/CeO₂/ZnO nanostructure and pure ZnO.

degradation reaction. Therefore, these results show smaller amount of degradation efficiency [13,15,29,30]. The objective of this work is to synthesize a novel nanostructure which can be used to degrade dyes and industrial textile effluent under visible light irradiation and minimize the irradiation time compared with ZnO/Ag (degradation of MB within 120min) and ZnO/CeO₂ (degradation of MB within 150min) which were previously reported [13,15]. The photocatalytic degradation of initially mixed solution (dye+catalyst), and the uniform irradiation time of MB, MO and industrial textile effluent and their corresponding UV-vis absorption spectrum are shown in Fig. 6.

The UV-vis absorption results evidently showed that when the irradiation time increases, the concentration of dyes decrease and finally gets straight line which means that the MO and MB has been degraded completely within 90min. The nanostructure degraded MB solution much faster when compared with binary ZnO/Ag and ZnO/CeO₂ nanocomposites [13,15]. On the other hand, while compared with CeO₂/C₃N₄, ZnO/CeO₂@HNTs, g-C₃N₄/CeO₂/ZnO and Ag₃PO₄/CeO₂ materials showing lowering rates [31–34]. The photocatalytic degradation rate depends on several parameters like method of synthesis of catalyst, morphology, size, crystallinity, bandgap, particle size, surface area and the availability of surface hydroxyl groups [13,15,31–34]. Furthermore, the colorless compound like phenol solution were carried for degradation process under visible light condition. The results (Fig. S4) were clearly exhibited the prepared material degrade the 98% of phenol solution within 120min.

For industrial textile effluent degradation, the rate of degradation of MB and MO is better due to its simple structure and also the industrial textile effluent contains lot of colored dyes, this statement was in good agreement with the recent literatures [35]. The recycling process of industrial textile effluent (Fig. 6d) results indicates that the ternary Ag/CeO₂/ZnO nanostructure have

good stability. Thus, the nanostructure is usable for long term environmental remediation process.

Fig. 7 represents the photocatalytic pathway mechanism for the ternary Ag/CeO₂/ZnO nanostructure under visible light irradiation. This ternary system have two semiconductors ZnO, and CeO₂ as well as metallic Ag having different work functions i.e. 5.20eV [13,20], 4.69eV [18,21] and 4.26eV [13,18,20], respectively. In general, when the semiconductor interacts with metal, Schottky barrier is formed and induced the new fermi level [13,20,36]. Therefore, the ternary Ag/CeO₂/ZnO nanostructure forms new fermi energy level and has lot of free electrons due to the presence of metallic Ag [13,20]. During the photocatalytic degradation, when the visible light falls on the surface of the ternary Ag/CeO₂/ZnO nanostructure, free electrons are excited due to surface plasmon resonance (SPR) mechanism, the excited electrons are transferred into the conduction band of CeO₂ and ZnO simultaneously [13,20]. The conduction band electrons and other free electrons react with adsorbed oxygen molecules during the reaction process and get converted into superoxide anion [8]. This superoxide anion reacts with water molecules and finally forms hydroxide radicals. These radicals effectively degrade the colored dyes and industrial textile effluents under visible light irradiation.

Moreover, Ag/CeO₂/ZnO photocatalyst having oxygen vacancies and Ce³⁺ due to line defect generates intermediate states which induces narrowing of band gap which was confirmed by DRS and HR-TEM results^{37–39}. Thus, oxygen vacancies and Ce³⁺ lead to improve the visible light induced photocatalytic degradation through harvesting maximum amount of visible light in short time. The similar statement has been reported by several other authors [6,8,37,38]. Therefore, we too assume that the ternary Ag/CeO₂/ZnO nanostructure shows excellent efficiency for the degradation of dyes as well as industrial textile effluent owing

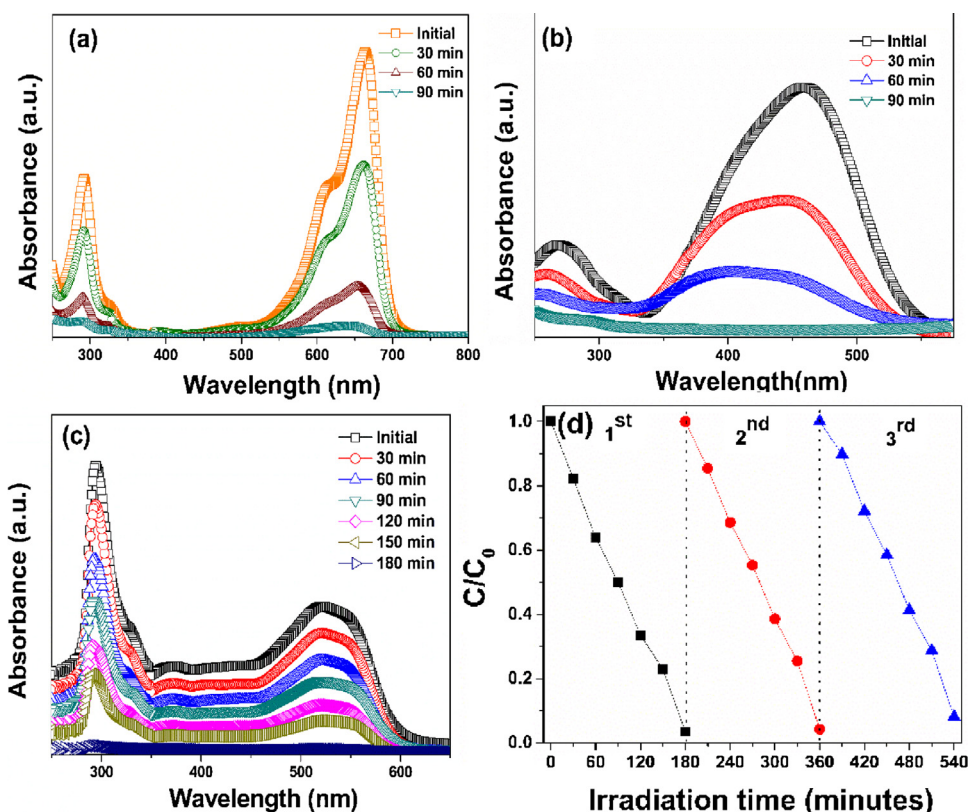
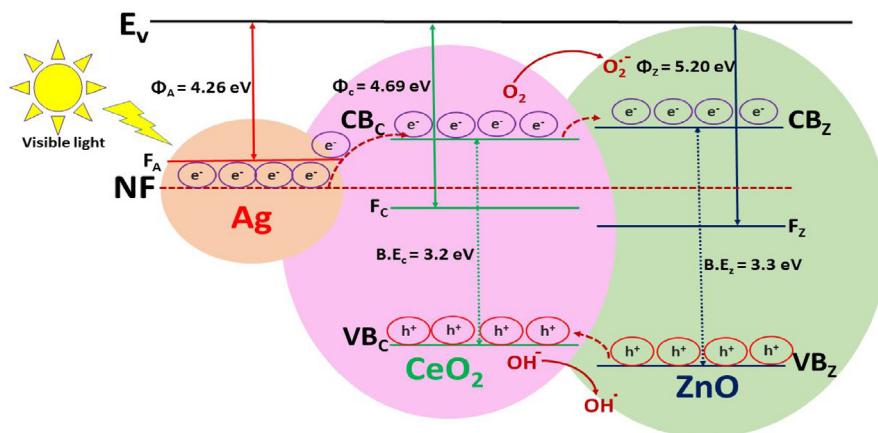


Fig. 6. UV-vis absorption spectra of photocatalytic degradation of (a) MB, (b) MO, (c) industrial textile effluent, and, (d) recycling process of industrial textile effluent using ternary Ag/CeO₂/ZnO nanostructure.



E_v = Energy in vacuum; Φ = Work function; NF = New Fermi Energy; F = Fermi Energy; A = Ag; C = CeO₂; Z = ZnO and B.E = Band Gap Energy.

Fig. 7. Schematic diagram representing the electron flow and photocatalytic degradation mechanism of pollutants using ternary Ag/CeO₂/ZnO nanostructure.

to the Ag, Ce³⁺ and oxygen vacancies present in this system, which would be helpful to improve the photocatalytic degradation activity of the ternary Ag/CeO₂/ZnO nanostructure under visible light irradiation [6,8,13,36,39,40–47].

4. Conclusion

The ternary Ag/CeO₂/ZnO nanostructure was successfully synthesized by thermal decomposition method, characterized by standard techniques (DRS, XRD, XPS, STEM and HR-TEM) and tested for visible light-induced photocatalytic degradation of colored dyes and industrial textile effluent (real sample analysis) as well as recycling process. The synthesized ternary Ag/CeO₂/ZnO nanostructure showed hexagonal and cubic phases which were confirmed by XRD whereas XPS analysis confirms the presence of Ag, Ce⁴⁺, Ce³⁺, Zn²⁺ and O. The XPS and HR-TEM results also confirms the line dislocation linear defect induced oxygen vacancy in the ternary Ag/CeO₂/ZnO nanostructure. The oxygen vacancy creates narrow band gap (2.66 eV), which was further confirmed by DRS. The oxygen vacancy promotes intermediate states which induces narrow band gap. The narrow band gap helps to excite the ternary Ag/CeO₂/ZnO nanostructure in visible light and produces sufficient electrons and holes for the photocatalytic degradation reactions. The intermediate state of the ternary Ag/CeO₂/ZnO nanostructure inhibited the electron-hole recombination, which results in superior photocatalytic activity. The ternary Ag/CeO₂/ZnO nanostructure showed outstanding photocatalytic activity in short period of visible light irradiation because of the narrow band gap, surface plasmon resonance (SPR) of Ag nanoparticles, synergistic effects, and defects (Ce³⁺ and oxygen vacancy) in CeO₂ and ZnO.

Acknowledgement

We acknowledge the Department of Nuclear Physics and National Centre for Nanoscience and Nanotechnology, University of Madras, India for XRD and XPS characterizations.

Appendix A. Supplementary data

Supplementary data associated with this article can be found, in the online version, at <https://doi.org/10.1016/j.jphotochem.2017.12.011>.

References

- [1] G. Reiss, A. Hutten, Magnetic nanoparticles: applications beyond data storage, *Nat. Mater.* 4 (2005) 725–726.
- [2] Z. Nie, A. Petukhova, E. Kumacheva, Properties and emerging applications of self-assembled structures made from inorganic nanoparticles, *Nat. Nanotechnol.* 5 (2010) 15–25.
- [3] R.A. Petros, J.M. DeSimone, Strategies in the design of nanoparticles for therapeutic applications, *Nat. Rev. Drug Discov.* 9 (2010) 615–627.
- [4] V.K. Gupta, I. Ali, T.A. Saleh, A. Nayak, S. Agarwal, Chemical treatment technologies for waste-Water recycling—an overview, *RSC Adv.* 2 (2012) 6380–6388.
- [5] M.R. Hoffmann, S.T. Martin, W. Choi, D.W. Bahnemann, Environmental applications of semiconductor photocatalysis, *Chem. Rev.* 95 (1995) 69–96.
- [6] S.A. Ansari, M.M. Khan, M.O. Ansari, J. Lee, M.H. Cho, Band gap engineering of CeO₂ nanostructure by electrochemically active biofilm for visible light applications, *RSC Adv.* 4 (2014) 16782–16791.
- [7] A. Fujishima, K. Honda, Electrochemical photolysis of water at a semiconductor electrode, *Nature* 238 (1972) 37–38.
- [8] M.M. Khan, S.A. Ansari, D. Pradhan, D.H. Han, J. Lee, M.H. Cho, Defect-Induced band gap narrowed CeO₂ nanostructures for visible light activities, *Ind. Eng. Chem. Res.* 53 (2014) 9754–9763.
- [9] M.M. Khan, S.F. Adil, A. Mayouf, A metal oxides as photocatalysts, *J. Saudi Chem. Soc.* 19 (2015) 462–464.
- [10] M. Arakha, M. Saleem, B.C. Mallick, S. Jha, The effects of interfacial potential on antimicrobial propensity of ZnO nanoparticle, *Nature Sci. Rep.* 5 (9578) (2015) 1–10.
- [11] R. Saravanan, V.K. Gupta, V. Narayanan, A. Stephen, Comparative study on photocatalytic activity of ZnO prepared by different methods, *J. Mol. Liquids.* 181 (2013) 133–141.
- [12] P.K. Shrestha, Y.T. Chun, D. Chu, A high-Resolution optically addressed spatial light modulator based on ZnO nanoparticles, *Nature Light: Sci. Appl.* 4 (2015) 1–7 (e259).
- [13] R. Saravanan, N. Karthikeyan, V.K. Gupta, P. Thangadurai, V. Narayanan, A. Stephen, ZnO/Ag nanocomposite an efficient catalyst for degradation studies of textile effluents under visible light, *Mater. Sci. Eng. C* 33 (2013) 2235–2244.
- [14] Q. Yu, J. Li, H. Li, Q. Wang, S. Cheng, L. Li, Fabrication, structure, and photocatalytic activities of boron-doped ZnO nanorods hydrothermally grown on CVD diamond film, *Chem. Phys. Lett.* 539 (2012) 74–78.
- [15] R. Saravanan, N. Karthikeyan, S. Govindan, V. Narayanan, A. Stephen, Photocatalytic degradation of organic dyes using ZnO/CeO₂ nanocomposite material under visible light, *Adv. Mater. Res.* 584 (2012) 381–385.
- [16] M.M. Khan, S.A. Ansari, J.H. Lee, M.O. Ansari, J. Lee, M.H. Cho, Electrochemically active biofilm assisted synthesis of Ag@CeO₂ nanocomposites for antimicrobial activity, photocatalysis and photoelectrodes, *J. Colloid Interface Sci.* 431 (2014) 255–263.
- [17] P.X. Huang, F. Wu, B.L. Zhu, X.P. Gao, H.Y. Zhu, T.Y. Yan, W.P. Huang, S.H. Wu, D.Y. Song, CeO₂ nanorods and gold nanocrystals supported on CeO₂ nanorods as catalyst, *J. Phys. Chem. B* 10 (2005) 19169–19174.
- [18] Y. Zheng, C. Chen, Y. Zhan, X. Lin, Q. Zheng, K. Wei, J. Zhu, Photocatalytic activity of Ag/ZnO heterostructure nanocatalyst: correlation between structure and property, *J. Phys. Chem. C* 112 (2008) 10773–10777.
- [19] S.S. Warule, N.S. Chaudhari, B.B. Kale, K.R. Patil, P.M. Koinkar, M.A. More, R. Murakami, Organization of cubic CeO₂ nanoparticles on the edges of self-Assembled tapered ZnO nanorods via a template free one-Pot synthesis:

- significant cathode luminescence and field emission properties, *J. Mater. Chem.* 22 (2012) 8887–8895.
- [20] J. Mu, C. Shao, Z. Guo, Z. Zhang, M. Zhang, P. Zhang, B. Chen, Y. Liu, High photocatalytic activity of ZnO-Carbon nanofiber hetero architectures, *ACS Appl. Mater. Interfaces.* 3 (2011) 590–596.
- [21] K. Jayanthi, S. Chawla, K.N. Sood, M. Chhibara, S. Singh, Dopant induced morphology changes in ZnO nanocrystals, *Appl. Surf. Sci.* 255 (2009) 5869–5875.
- [22] L. Sun, D. Marrocchelli, B. Yildiz, Edge dislocation slows down oxide ion diffusion in doped CeO₂ by segregation of charged defects, *Nat. Commun.* 6 (6294) (2015) 1–10.
- [23] Y. Yang, C. Sun, L. Wang, Z. Liu, G. Liu, X. Ma, H.M. Cheng, Constructing a Metallic/Semiconducting TaB₂/Ta₂O₅ Core/Shell heterostructure for photocatalytic hydrogen evolution, *Adv. Energy Mater.* 4 (1400057) (2014) 1–7.
- [24] H. Wang, S. Baek, J. Lee, S. Lim, High photocatalytic activity of silver-Loaded ZnO-SnO₂ coupled catalysts, *Chem. Eng. J.* 146 (2009) 355–361.
- [25] Y. Yang, Y. Yang, L.C. Yin, X. Kang, G. Liu, H.M. Cheng, An amorphous carbon nitride photocatalyst with greatly extended visible-Light-Responsive range for photocatalytic hydrogen generation, *Adv. Mater.* 27 (2015) 4572–4577.
- [26] B. Tatar, E.D. Sam, K. Kutlu, M. Urgan, Synthesis and optical properties of CeO₂ nanocrystalline films grown by pulsed electron beam deposition, *J. Mater. Sci.* 43 (2008) 5102–5108.
- [27] R. Saravanan, H. Shankar, T. Prakash, V. Narayanan, A. Stephen, ZnO/CdO composite nanorods for photocatalytic degradation of methylene blue under visible light, *Mater. Chem. Phys.* 125 (2011) 277–280.
- [28] R. Saravanan, V.K. Gupta, V. Narayanan, A. Stephen, Visible light degradation of textile effluent using novel catalyst ZnO/γ-Mn₂O₃, *J. Taiwan Inst. Chem. Eng.* 45 (2014) 1910–1917.
- [29] R. Saravanan, M.M. Khan, V.K. Gupta, E. Mosquera, F. Gracia, V. Narayanan, A. Stephen, ZnO/Ag/CdO nanocomposite for visible light-Induced photocatalytic degradation of industrial textile effluents, *J. Colloid Interface Sci.* 452 (2015) 126–133.
- [30] D.B. Suyatin, et al., Strong schottky barrier reduction at Au-Catalyst/GaAs-Nanowire interfaces by electric dipole formation and fermi-Level unpinning, *Nat. Commun.* 5 (3221) (2014) 1–8.
- [31] Y. Yuan, et al., Construction of g-C₃N₄/CeO₂/ZnO ternary photocatalysts with enhanced photocatalytic performance, *J. Phys. Chem. Solids* 106 (2017) 1–9.
- [32] Z. Ye, et al., Well-dispersed nebula-like ZnO/CeO₂@HNTs heterostructure for efficient photocatalytic degradation of tetracycline, *Chem. Eng. J.* 304 (2016) 917–933.
- [33] Z.M. Yang, et al., Novel Ag₃PO₄/CeO₂ composite with high efficiency and stability for photocatalytic applications, *J. Mater. Chem. A* 2 (2014) 1750–1756.
- [34] D.F. Li, et al., Enhancement of photocatalytic activity of combustion-synthesized CeO₂/C₃N₄ nanoparticles, *Appl Phys. A* 120 (2015) 1205–1209.
- [35] J. Wang, Z. Wang, B. Huang, Y. Ma, Y. Liu, X. Qin, X. Zhang, Y. Dai, Oxygen vacancy induced band-Gap narrowing and enhanced visible light photocatalytic activity of ZnO, *ACS Appl Mater. Interfaces.* 4 (2012) 4024–4030.
- [36] L.Y. Chen, M. He, J. Shin, G. Richter, D.S. Gianola, Measuring surface dislocation nucleation in defect-scarce nanostructures, *Nat. Mater.* 14 (2015) 707–713.
- [37] M. Aslam, M.T. Qamara, M.T. Soomroa, I.M.I. Ismail, N. Salahc, T. Almeelbi, M.A. Gondal, A. Hameed, The effect of sunlight induced surface defects on the photocatalytic activity of nanosized CeO₂ for the degradation of phenol and its derivatives, *Appl. Catal B: Environ.* 180 (2016) 391–402.
- [38] S.I. Cha, K.H. Hwang, Y.H. Kim, M.J. Yun, S.H. Seo, Y.J. Shin, J.H. Moon, D.Y. Lee, Enhanced photocatalytic behavior of TiO₂ rutile nano-belts induced by dislocations, *Nanoscale* 5 (2013) 753–758.
- [39] Z.W. Pan, Z.R. Dai, Z.L. Wang, Nanobelts of semiconducting oxides, *Science* 291 (2001) 1947–1949.
- [40] G. Chen, L. Lei, P.L. Yue, Wet oxidation of high-concentration reactive dyes, *Ind. Eng. Chem. Res.* 38 (1999) 1837–1843.
- [41] R. Saravanan, S. Karthikeyan, V.K. Gupta, G. Sekaran, V. Narayanan, A. Stephen, *Mat. Sci. Engineering: C* 33 (2013) 91–98.
- [42] M. Ahmaruzzaman, V.K. Gupta, Rice husk and its ash as low-cost adsorbents in water and wastewater treatment, *Ind. Eng. Chem. Res.* 50 (2011) 13589–13613.
- [43] S. Karthikeyan, V.K. Gupta, R. Boopathy, A. Titus, G. Sekaran, A new approach for the degradation of aniline by mesoporous activated carbon as a heterogeneous catalyst: kinetic and spectroscopic studies, *J. Mol. Liquids* 173 (2012) 153–163.
- [44] T.A. Saleh, V.K. Gupta, Synthesis and characterization of alumina nanoparticles polyamide membrane with enhanced flux rejection performance, *Sep. Purif. Technol.* 89 (2012) 245–251.
- [45] Tawfik A. Saleh, Shilpi Agarwal, V.K. Gupta, Synthesis of MWCNT/MnO₂ Composites and their application for simultaneous oxidation of arsenite and sorption of arsenate, *Applied Catalysis B: Environ.* 106 (2011) 46–53.
- [46] V.K. Gupta, Necip Atar, M.L. Yola, Zafer Üstündağ, Lokman Uzun, A novel magnetic Fe@Au core-shell nanoparticles anchored graphene oxide recyclable nanocatalyst for the reduction of nitrophenol compounds, *Water Res.* 48 (2014) 210–217.
- [47] V.K. Gupta, A. Nayak, S. Agarwal, Bioadsorbents for remediation of heavy metals: current status and their future prospects, *Environ. Eng. Res.* 20 (1) (2015) 001–018.